JB
Journals.ASM.org

# MexT Functions as a Redox-Responsive Regulator Modulating Disulfide Stress Resistance in *Pseudomonas aeruginosa*

**Emilie Fargier,[a,b]* Micheál Mac Aogáin,[a,b] Marlies J. Mooij,[a,b,c] David F. Woods,[a,b] John P. Morrissey,[b,c] Alan D. W. Dobson,[b,c] Claire Adams,[a] and Fergal O'Gara[a,b,c]**

BIOMERIT Research Centre, Department of Microbiology, University College Cork, Cork, Ireland[a]; Department of Microbiology, University College Cork, Cork, Ireland[b]; and Marine Biotechnology Centre, Environmental Research Institute, University College Cork, Cork, Ireland[c]

**MexT is a global LysR transcriptional regulator known to modulate antibiotic resistance and virulence in *Pseudomonas aeruginosa*. In this study, a novel role for MexT in mediating intrinsic disulfide stress resistance was demonstrated, representing the first identified phenotype associated with inactivation of this regulator in wild-type cells. Disruption of *mexT* resulted in increased susceptibility to the disulfide stress elicitor diamide [diazenedicarboxylic acid bis(*N*,*N*,-di-methylamide)]. This compound is known to elicit a specific stress response via depletion of reduced glutathione and alteration of the cellular redox environment, implicating MexT in redox control. In support of this, MexT-regulated targets, including the MexEF-OprN multidrug efflux system, were induced by subinhibitory concentrations of diamide. A *mexF* insertion mutant also exhibited increased diamide susceptibility, implicating the MexEF-OprN efflux system in MexT-associated disulfide stress resistance. Purified MexT protein was observed to form an oligomeric complex in the presence of oxidized glutathione, with a calculated redox potential of −189 mV. This value far exceeds the thiol-disulfide redox potential of the bacterial cytoplasm, ensuring that MexT remains reduced under normal physiological conditions. MexT is activated by mutational disruption of the predicted quinone oxidoreductase encoded by *mexS*. Alterations in the cellular redox state were observed in a *mexS* mutant (PA14*nfxC*), supporting a model whereby the perception of MexS-associated redox signals by MexT leads to the induction of the MexEF-OprN efflux system, which, in turn, may mediate disulfide stress resistance via efflux of electrophilic compounds.**

*Pseudomonas aeruginosa* is a major clinical pathogen and the most common cause of morbidity and mortality in cystic fibrosis patients (13, 20). The genome of *P. aeruginosa* harbors a large number of transcriptional regulators, many of which modulate expression of virulence factors involved in the infection process (14, 15, 21, 63). MexT is a LysR-type transcriptional regulator (LTTR), which activates expression of the MexEF-OprN multidrug efflux system. Induction of MexEF-OprN leads not only to increased antibiotic resistance but also to repression of the quorum sensing cascade and several virulence factors (23, 24, 36). Due to its pleiotropic effect on *P. aeruginosa* physiology, MexT has been the subject of intense investigation (4, 8, 23, 24, 29). In addition to MexEF-OprN, several MexT-regulated target genes in *P. aeruginosa* have been identified, highlighting the role of MexT as a global transcriptional regulator (66). Interestingly, not all MexT-associated phenotypes are dependent on MexEF-OprN, and other members of the MexT regulon have come into focus as potential players in pathogen-host interactions (9, 19, 66, 67). The molecular mechanism by which MexT activates expression of its targets is thus an important physiological process in the context of understanding *P. aeruginosa* pathogenesis.

LysR-type transcriptional regulators require the presence of a coinducer to activate their target genes (41, 56). Several LTTRs are known to activate gene expression as higher oligomeric complexes, which form on recognition of their cognate signals (2, 53, 55, 57). Studies on the classical LysR regulator OxyR, which forms oligomeric complexes when oxidized, suggest that a subset of LTTRs are activated via a redox-sensing mechanism (2, 69, 70, 72). MexT is quiescent in wild-type *P. aeruginosa* cells, suggesting that the MexT coinducer is absent or present at low concentrations under standard laboratory growth conditions (60, 67). However, MexT is known to become constitutively active in spontaneously arising mutants termed *nfxC* mutants, so called because of their original isolation in the presence of the fluoroquinolone antibiotic norfloxacin (nfx) (17, 23, 60). Although several mutations may cause MexEF-OprN induction, the most frequently reported are inactivating mutations in the *mexS* gene (38, 60). Inactivation of *mexS* (a gene divergently transcribed from *mexT* encoding a putative oxidoreductase) leads to constitutive activation of MexT, suggesting that MexS and MexT are functionally linked (19, 60). It has been postulated that MexS is involved in the detoxification of an endogenously produced, MexT-activating molecule (52). Furthermore, a recent study suggests that MexEF-OprN offers protection from endogenous metabolic stressors (28). MexT is activated by the nitrosative stress elicitors *S*-nitrosoglutathione (GNSO) and diethylaminetriamine NONOate (DETA) as well as the antibiotic chloramphenicol, and transcriptome analysis has revealed that the MexT regulon is induced in response to airway epithelial cells (9, 11). This has led to the hypothesis that MexT is activated *in vivo* and serves a physiological function related to pathogen-host interactions (9, 60, 66). In addition, mutations in both *mexT* and *mexS* are common in clinical isolates and occur during colonization of the cystic fibrosis lung (38, 59). However,

**Received** 13 December 2011 **Accepted** 3 April 2012
**Published ahead of print** 27 April 2012
Address correspondence to Fergal O'Gara, f.ogara@ucc.ie.
* Present address: Emilie Fargier, Biocodex, Compiègne, France.
E.F. and M.M.A. contributed equally to this article.
Supplemental material for this article may be found at http://jb.asm.org/.

doi:10.1128/JB.06632-11

**TABLE 1** Strains and plasmids used in this study

| Strain or plasmid | Description[a] | Reference or source |
|---|---|---|
| Strains | | |
| PA14 | Wild-type lab stock | 33 |
| PA14*nfxC* | PA14 *mexEF-oprN*-overexpressing strain harboring a spontaneous mutation in *PA14_32420* (*mexS*) | 46 |
| PA14::*mexT* | PA14 harboring mariner Tn*7* transposon insertion in *PA14_32410* (*mexT*); $Gm^r$ | 33 |
| PA14::*mexE* | PA14 harboring mariner Tn*7* transposon insertion in *PA14_32400* (*mexE*); $Gm^r$ | 33 |
| PA14::*mexF* | PA14 harboring mariner Tn*7* transposon insertion in *PA14_32390* (*mexF*); $Gm^r$ | 33 |
| PA14::*oprN* | PA14*nfxC* harboring mariner Tn*7* transposon insertion in *PA14_32380* (*oprN*); $Gm^r$ | 33 |
| PA14*nfxC*::*mexT* | PA14*nfxC* harboring Tn*5* transposon insertion in *PA14_32410* (*mexT*); $Tc^r$ | This study |
| PA14*nfxC*::*mexF* | PA14*nfxC* harboring Tn*5* transposon insertion in *PA14_32390* (*mexF*); $Tc^r$ | This study |
| PA14*nfxC*::*oprN* | PA14*nfxC* harboring Tn5 transposon insertion in *PA14_32380* (*oprN*); $Tc^r$ | This study |
| *E. coli* DH5α | $F^-$ φ80 *lacZ*ΔM15 (Δ*lacZYA-argF*)*U169 deoR recA1 endA1 hsdR17*($r_K^-$ $m_K^-$) *phoA supE44 thi-1 gyrA96 relA1*Δ$^-$ | Invitrogen |
| *E. coli* S17-1 λ$^-$ pir (pUTmini-Tn*5*-luxCDABE-Tc) | λ lysogenic S17-1 derivative harboring pUTmini-Tn*5*- luxCDABE-Tc transposon delivery vector; $Tc^r$ | 31 |
| BL21-CodonPlus (DE3)-RIPL | Protein expression host; $Cm^r$ $Str^r$ | Merck |
| Plasmids | | |
| pRK2013 | $Tra^+$ $Mob^+$, ColE1 replicon; $Km^r$ | 10 |
| pME6032 | pVS1-p15A origin, *lacI*$^q$-P*tac* expression vector; $Tc^r$ | 16 |
| pME-mexTNP | pME6032-derived *mexT* expression vector | This study |
| pBBR1MCS5 | Broad-host-range cloning vector; $Gm^r$ | 26 |
| pBBR-mexS | pBBR1MCS5-derived *mexS* expression vector | This study |
| pMP190 | *IncQ* origin, low-copy-number *lacZ* fusion vector; $Cm^r$ $Str^r$ | 61 |
| pMP-PA4881p | pMP190-derived PAO1 *PA4881* promoter-*lacZ* fusion plasmid | 66 |
| pMP-PAmexEp | pMP190-derived PAO1 *mexE* promoter-*lacZ* fusion plasmid | 66 |
| pMP-PA4354p | pMP190-derived PAO1 *PA4354* promoter-*lacZ* fusion plasmid | 66 |
| pETmexTH6C | pET28a-derived C-terminal His6-tag MexT expression vector; $Km^r$ | 66 |

[a] $Gm^r$, gentamicin resistance; $Tc^r$, tetracycline resistance; $Km^r$, kanamycin resistance; $Cm^r$, chloramphenicol resistance; $Str^r$, streptomycin resistance.

no phenotype has yet been associated with disruption of *mexT* or *mexEF-oprN* in wild-type *P. aeruginosa* cells.

In this study, we investigated the role of MexT in mediating disulfide stress resistance, which represents a novel MexT-associated phenotype. The role of MexT in protecting against redox imbalances generated by the disulfide stress elicitor diamide [diazenedicarboxylic acid bis(*N*,*N*,-di-methylamide)] was determined, and the ability of diamide to induce MexT-regulated targets was investigated. Disulfide stress is a subcategory of oxidative stress caused by perturbation of the thiol-disulfide balance in the cytoplasm, which can arise due to the accumulation of thiol-reactive compounds such as quinones (34, 58). Diamide reacts readily with free thiols, causing thiol-disulfide imbalances in the cytoplasm and the formation of aberrant disulfide bonds (25, 58). Diamide thus simulates stress-inducing redox imbalances caused by naturally occurring electrophiles. Importantly, diamide does not participate in the generation of radicals, which differentiates it from other oxidative stress elicitors such as $H_2O_2$. Thus, the physiological response elicited by diamide is clearly distinct from that of $H_2O_2$ and involves alternative regulatory networks (22, 25, 30, 51). Here we demonstrate that MexT is a crucial redox-responsive regulator mediating intrinsic disulfide stress resistance in *P. aeruginosa*, the activation of which is triggered by changes in the thiol-disulfide redox state.

## MATERIALS AND METHODS

**Strains and plasmids.** The strains and plasmids used in this study are listed in Table 1. Several mutants from the PA14 nonredundant (NR) transposon insertion library (33) were also surveyed in this study and are listed in Table S1 in the supplemental material, which also contains the primers used to reconfirm the location of transposon insertions in these strains. The spontaneously generated MexEF-OprN-overexpressing strain PA14*nfxC* was shown to be a *mexS* mutant by complementation and sequence analysis. All strains were routinely cultured in Luria-Bertani (LB) broth at 37°C with shaking at 150 rpm. Plasmids were transferred from *Escherichia coli* DH5α into PA14 by triparental mating using helper plasmid pRK2013 (10). Antibiotics were added to cultures where required at the following concentrations: for *E. coli*, kanamycin at 25 μg $ml^{-1}$, gentamicin at 10 μg $ml^{-1}$, chloramphenicol at 20 μg $ml^{-1}$, and tetracycline at 10 μg $ml^{-1}$; and for *P. aeruginosa*, streptomycin at 100 μg $ml^{-1}$, gentamicin at 25 μg $ml^{-1}$, and tetracycline at 25 μg $ml^{-1}$.

**Disk diffusion and broth microdilution sensitivity assays.** The sensitivity of *P. aeruginosa* to $H_2O_2$, diamide, chloramphenicol, and tetrazolium violet (TV; 2,5-diphenyl-3-2-naphthyl tetrazolium chloride) (Sigma, United Kingdom) was assessed by disk diffusion. Each compound was added to filter paper disks and allowed to dry at room temperature. The concentrations of each compound per disk were 90 μg for $H_2O_2$, 1 mg for diamide, 100 μg for chloramphenicol, and 2 mg for tetrazolium violet. A bacterial lawn was inoculated onto LB agar using sterile swabs from a standardized cell suspension of each strain (optical density [OD] at 600 nm = 0.125). Filter paper disks containing each compound were then added to inoculated plates and incubated at 37°C for 16 h, and zones of inhibition were compared. The MIC of diamide and chloramphenicol was also determined by broth microdilution. Briefly, a dilution series of diamide was made up in 100 μl of LB broth dispensed in 96-well plates. Wells were inoculated with between $10^4$ and $10^5$ CFU $ml^{-1}$ of bacterial culture and incubated statically for 24 h at 37°C. The diamide MIC was defined as the lowest concentration at which no growth was visible after 24 h.

**Generation of *mexT*- and *mexS*-complementing plasmids.** In order to complement phenotypes associated with disruption of *mexS* and *mexT*

in PA14*nfxC* and PA14::*mexT*, respectively, the complementation constructs pBBR-mexS and pME-mexTNP were generated. A 1-kb fragment including the *mexS* coding region was ligated into the HindIII and XbaI restriction sites of pBBR1MCS5 to yield the constitutive *mexS* expression construct pBBR-mexS. Similarly, a 0.9-kb fragment encompassing the *mexT* coding sequence was cloned into the EcoRI and KpnI sites of the pME6032 multiple cloning site to yield the isopropyl-β-D-thiogalactopyranoside (IPTG)-inducible *mexT* overexpression construct pME-mexTNP.

**Tn*5* mutagenesis of PA14*nfxC*.** To generate transposon insertions in *mexT* and *mexEF-oprN* in the PA14*nfxC* background, a Tn*5* mutagenesis approach was taken. Random mini-Tn*5* mutagenesis was used to generate mutants in PA14*nfxC* (which is highly chloramphenicol resistant due to the constitutive induction of MexEF-OprN) using the mini-Tn*5*-*luxCDABE* construct as previously described (31). Following mini-Tn*5* mutagenesis, individual colonies were transferred to M9-citrate containing chloramphenicol at 200 μg ml$^{-1}$ (a concentration inhibitory to PA14 but permissive to PA14*nfxC*). This allowed the identification of mutants in which chloramphenicol susceptibility was restored to wild-type levels. The locations of Tn*5* insertions were mapped in several candidates using a previously described protocol (31). Mutants in the PA14*nfxC* background with insertions in *mexT*, *mexF*, and *oprN* (PA14*nfxC*::*mexT*, PA14*nfxC*::*mexF*, and PA14*nfxC*::*oprN*, respectively) were generated by this approach. The primers and PCR conditions used to map transposon insertions are detailed in Tables S2 and S3 in the supplemental material.

**Diamide induction assay.** PA14 strains harboring *lacZ* reporter fusions were grown overnight at 37°C in 5 ml of LB broth with appropriate antibiotic selection. Cultures were diluted to an optical density of 0.02 at 600 nm in 5 ml of LB broth without diamide, LB broth containing 8 mM diamide, or LB broth containing 16 mM diamide in 6-well polystyrene tissue culture plates (Sarstedt, United Kingdom) in the presence of 100 μg ml$^{-1}$ streptomycin. Cultures were grown with shaking (150 rpm) at 37°C for 24 h. The β-galactosidase activity present in each culture was quantified and expressed as Miller units (45).

**Redox titration of MexT.** His-tagged MexT protein was purified to homogeneity by nickel affinity chromatography as previously described (66). Purified protein was analyzed by SDS-PAGE under oxidizing and reducing conditions to assess whether oligomerization of MexT could be observed. Purified protein was incubated in defined concentrations of reduced glutathione (GSH) and oxidized glutathione (GSSG)—0 to 5.5 mM for GSH and 0.3 mM for GSSG—for 2 h. The reaction was then stopped by adding an excess of iodoacetamide and incubating the protein at 37°C for 30 min to alkylate free thiols. The ratio of oxidized versus reduced MexT was visualized by nonreducing denaturing SDS-PAGE and staining with Coomassie brilliant blue dye. MexT was also analyzed under fully reducing conditions in the presence of 100 mM dithiothreitol (DTT). A redox titration curve was generated for MexT, assuming a concerted four-monomer oxidation and reduction involving eight-electron exchange (equation 1).

$$\mathrm{McxT(ox)} + 8\mathrm{GSH} \leftrightarrow \mathrm{MexT(red)} + 4\mathrm{GSSG} \quad (1)$$

The equilibrium constant of this reaction was calculated from the plotted redox titration curve (see Fig. 4b), and the redox potential of MexT was determined through application of the Nernst equation (1, 72).

**EMSAs.** DY-682 infrared-labeled primers (PA4881EF, 5′-CGGCTTTCTCTTTTCGCCTTA-3′; PA4881ER, 5′-TGCGTTGGAGTCATTTTCAG-3′; Eurofins MWG Operon, United Kingdom) were used to amplify a 207-bp fragment from the *PA4881* promoter region containing the previously characterized MexT binding site (66). Amplified fragments were purified using the Qiagen PCR purification kit (Qiagen, United Kingdom), and 10 fmol of each was used as a DNA probe in electrophoretic mobility shift binding assays (EMSAs). Labeled probes were incubated at 37°C for 45 min in the presence and absence of 12.5 ng of purified His-tagged MexT protein in binding buffer (20 mM Tris-HCl [pH 8], 60 mM KCl, 2.5 mM, $MgCl_2$, 1 mM EDTA [pH 8], 10% glycerol, 50 μg of bovine serum albumin [BSA]) which included 0.05 μg ml$^{-1}$ poly[d(I-C)] and 0.05 μg ml$^{-1}$ poly-L-lysine. Reactions were also performed in the presence of defined concentrations of GSH (0 to 5.5 mM) and GSSG (0.3 mM). Following incubation, samples were separated by electrophoresis on a 6% native polyacrylamide gel and were visualized on an Odyssey infrared imaging system (Li-COR Biosciences, United Kingdom).

**Tetrazolium violet reduction assay.** Reduction of TV to formazan in liquid cultures of PA14, PA14*nfxC*, and PA14*nfxC*::*mexF* harboring the pBBR-mexS construct was quantified as previously described and compared to that in the same strains harboring the pBBR1MCS5 vector control (64). For each strain, 200 μl of an overnight culture (adjusted to an optical density of 2 at 600 nm) was added to 25 ml of LB broth containing 25 μg ml$^{-1}$ gentamicin and TV at a final concentration of 0.01 mg ml$^{-1}$. After incubation for 24 h at 37°C, cells were promptly assayed for total formazan production. Five milliliters of culture was harvested by centrifugation (5,000 × *g*, 5 min), and the supernatant was removed. Cells were then resuspended in 1.2 ml of dimethyl sulfoxide to solubilize formazan precipitate in the pelleted cells. The cell suspension was centrifuged (5,000 × *g*, 5 min) and the absorbance of the cell-free supernatant was measured at 510 nm. For quantification, a calibration curve was established with a TV-formazan solution prepared as described elsewhere (64).

## RESULTS

**MexT confers disulfide resistance via the MexEF-OprN efflux system.** Previous studies have implicated both oxidative and nitrosative stress elicitors as inducing signals for MexT (9, 32). However, the absence of any MexT-associated oxidative or nitrosative stress-related phenotypes prompted us to investigate whether MexT conferred resistance to other redox stress elicitors. Although MexT has been speculated to respond to $H_2O_2$-induced stress signals, no difference in resistance to $H_2O_2$ between PA14 and the spontaneously generated MexEF-OprN-overexpressing strain PA14*nfxC* (*mexS* mutant) or the *mexT* disruption mutant PA14::*mexT* was observed by disk diffusion assay (data not shown). Hence, neither MexT nor MexEF-OprN appears to function in protecting the cell from the toxic effects of this reactive oxygen species. However, PA14*nfxC* did exhibit a slight increase in resistance to the disulfide stress elicitor diamide relative to its isogenic PA14 wild type (Fig. 1 and Table 2), suggesting that this efflux system might contribute to diamide resistance. More strikingly, the *mexT* insertion mutant PA14::*mexT* exhibited substantially increased susceptibility to diamide compared to its isogenic PA14 parent strain, indicating that MexT contributes to intrinsic diamide resistance (Fig. 1 and Table 2).

To investigate whether the MexEF-OprN efflux system, which is a direct regulatory target of MexT, was responsible for diamide resistance, PA14 strains taken from the nonredundant (NR) PA14 mutant library (33) harboring disrupted copies of *mexE*, *mexF*, or *oprN* were investigated. These mutants also exhibited increased susceptibility to diamide compared to their isogenic PA14 parent strain (Fig. 1 and Table 2), suggesting that MexT-associated diamide resistance is mediated via the MexEF-OprN tripartite efflux system. In support of this, complementation of *mexT* restored diamide susceptibility in PA14::*mexT* to wild-type levels, whereas the introduction of the pME-mexTNP construct into PA14::*mexF* had no impact on diamide susceptibility levels (see Fig. S1 in the supplemental material). Curiously, disruption of *oprN*, which encodes the outer membrane component of the MexEF-OprN efflux pump, had only a marginal impact on diamide susceptibility as determined by disk diffusion (Fig. 1). Furthermore, the PA14 *mexT*, *mexE*, and *mexF* mutants exhibited an 8-fold decrease in diamide MIC compared to the isogenic PA14 wild type, whereas

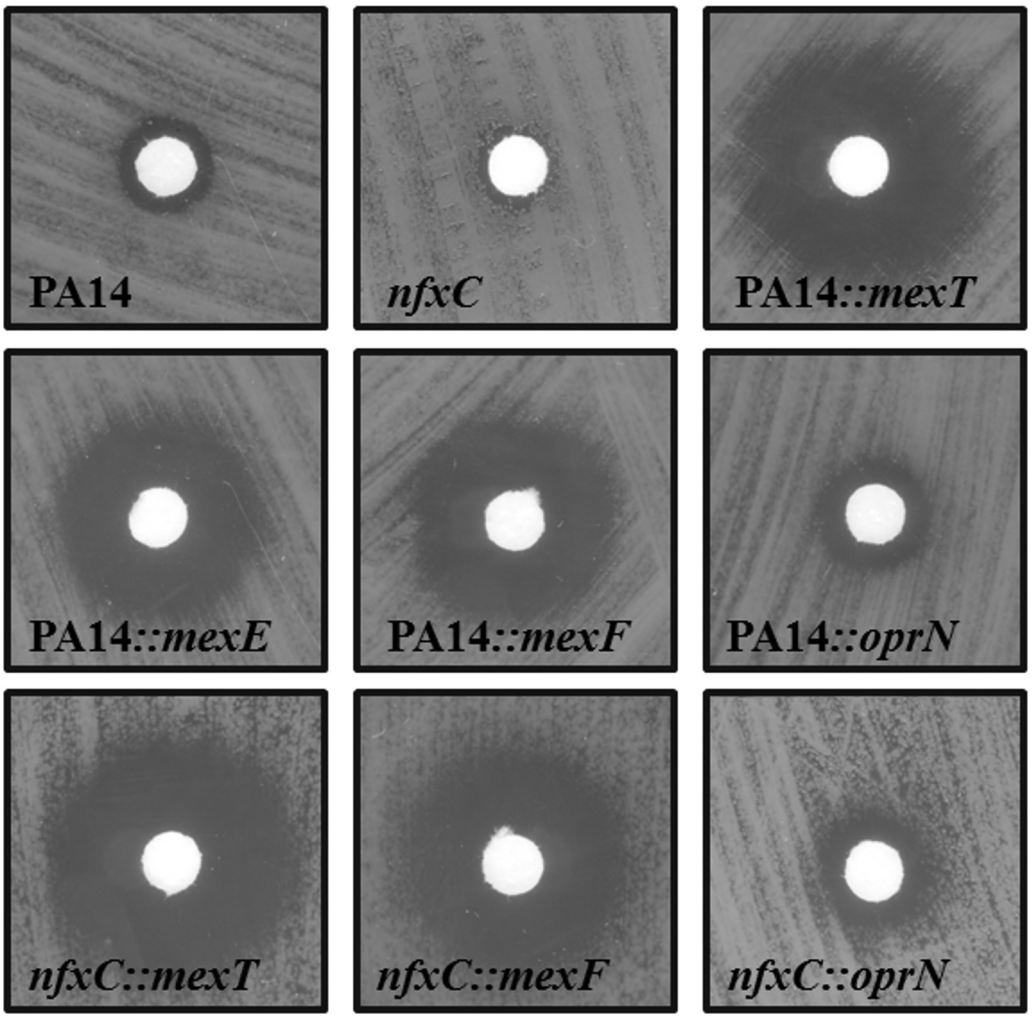


**FIG 1** Influence of MexT and MexEF-OprN on intrinsic diamide resistance. Diamide susceptibility was assessed by disk diffusion. Increased diamide resistance was observed in the *mexS* mutant PA14*nfxC* (*nfxC*) compared to PA14 as indicated by a small inhibitory zone around a diamide-containing disk in this mutant. Disruption of *mexT* led to markedly increased diamide susceptibility in PA14, observed as a large zone of inhibition surrounding the diamide disk in the case of the *mexT* insertion mutant PA14::*mexT*. PA14 insertion mutants PA14::*mexE* and PA14::*mexF* also exhibited larger inhibitory zones than did PA14. Disruption of *oprN* in PA14::*oprN* had a marginal effect on diamide susceptibility which was much less apparent than the effect seen in PA14::*mexT*, PA14::*mexE*, and PA14::*mexF* mutants. The diamide susceptibility phenotype was independently verified in a Tn*5* mutagenesis of *mexT* and *mexF* and in the PA14*nfxC* mutant. In PA14*nfxC*, Tn*5* disruption of *oprN* had a more marked impact on diamide resistance relative to its isogenic PA14*nfxC* wild-type parent than did Tn*7*-mediated disruption of *oprN* in PA14.

disruption of *oprN* had no effect on diamide susceptibility in liquid culture (Table 2).

To unequivocally validate the role of MexT and the MexEF-OprN efflux system in mediating intrinsic diamide resistance, PA14*nfxC*::*mexT*, PA14*nfxC*::*mexF*, and PA14*nfxC*::*oprN* double mutants, isolated through random Tn*5* mutagenesis of PA14*nfxC*, were tested for diamide resistance. Transposon mutagenesis of *mexT* and *mexF* in PA14*nfxC* not only abrogated the diamide resistance phenotype of PA14*nfxC* but also lowered diamide resistance to levels comparable with those of PA14::*mexT* and PA14::*mexF* (Fig. 1 and Table 2). However, while disruption of *oprN* restored the diamide sensitivity of PA14*nfxC* to wild-type levels, resistance was markedly higher than that observed for both PA14*nfxC*::*mexT* and PA14 *nfxC*::*mexF* (Fig. 1 and Table 2). This suggests that intrinsic diamide resistance is only partially dependent on OprN. Interestingly, phenazine production (which is strongly repressed in PA14*nfxC*) was restored in PA14*nfxC*::*mexT* and PA14*nfxC*::*mexF* but not in PA14*nfxC*::*oprN*. PA14*nfxC*::*oprN* also exhibited only partial restoration of chloramphenicol susceptibility (see Fig. S2 in the supplemental material). These observations correlate with our findings in the PA14 NR library

**TABLE 2** Determination of diamide MIC in PA14 mutants

| Strain | PA14 locus ID[a] | Diamide MIC (mM) |
|---|---|---|
| PA14 | | 32 |
| PA14::*mexT* | PA14_32410 | 4 |
| PA14::*mexE* | PA14_32400 | 4 |
| PA14::*mexF* | PA14_32390 | 4 |
| PA14::*oprN* | PA14_32380 | 32 |
| PA14*nfxC* | PA14_32420 (*mexS*) | 64 |
| PA14*nfxC*::*mexT* | PA14_32410 | 4 |
| PA14*nfxC*::*mexF* | PA14_32390 | 4 |
| PA14*nfxC*::*oprN* | PA14_32380 | 32 |

[a] The corresponding locus identity (ID) of mapped transposon insertions/mutations for *mexT*, *mexE*, *mexF*, *oprN*, and *mexS* in PA14 is indicated.

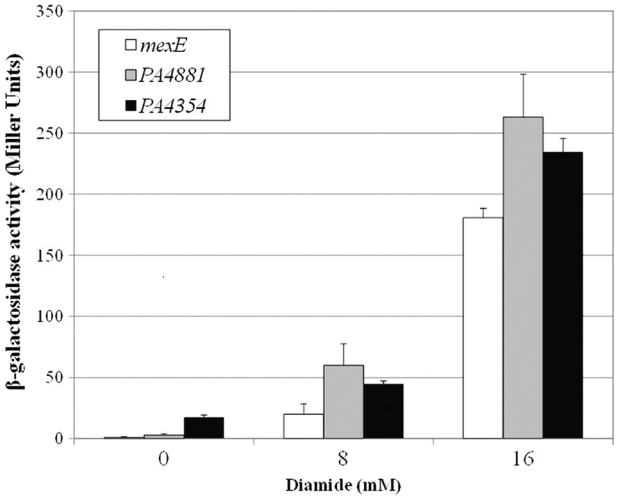


**FIG 2** Induction of MexT-regulated targets in the presence of diamide. The presence of 1/4 (8 mM) or 1/2 (16 mM) the diamide MIC of PA14 led to increased expression of *mexE*, *PA4881*, and *PA4354* compared to growth in the absence of diamide. Results from three biological replicates are presented, and error bars represent standard deviations. Expression from all promoter fusions was significantly induced in the presence of diamide ($P < 0.05$, two-tailed Student's *t* test).

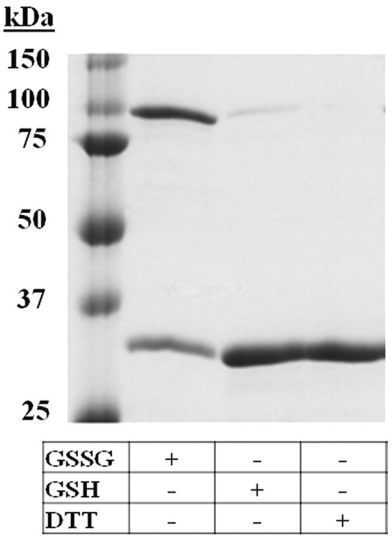


**FIG 3** His-tagged, purified MexT was observed to form an oligomeric complex under oxidizing conditions in the presence of GSSH (0.3 mM). Incubation of purified MexT protein in the presence of GSH (5.5 mM) led to the predominance of the MexT monomer and a decrease in the oligomeric MexT complex which was undetected under fully reducing conditions in the presence of DTT (100 mM).

mutants, in which diamide susceptibility was found to be largely independent of OprN.

To investigate whether other resistance nodulation division (RND) efflux systems or outer membrane porins might contribute to intrinsic diamide resistance, the susceptibility of mutants from the PA14 NR library was also assessed. Mutants with transposon insertions in each of the 11 additional RND efflux systems annotated in PA14 and their associated porins were surveyed for altered diamide susceptibility. However, all exhibited susceptibility comparable to that of the PA14 wild-type strain as determined by disk diffusion, suggesting that MexEF-OprN is distinguished among tripartite efflux systems in PA14 with respect to disulfide stress resistance (data not shown; surveyed mutants are listed in Table S1 in the supplemental material). The CzcC porin was not included in this survey, as it was not present in the PA14 NR library, and the PA14::*mexA* rather than the PA14::*mexB* mutant was used, as the *mexB* insertion could not be verified (see Table S1 in the supplemental material).

**MexT-regulated targets, including *mexEF-oprN*, are induced by diamide.** MexT has been demonstrated to regulate several targets in addition to *mexEF-oprN*, including the putative detoxification operon *PA4354-PA4355-xenB* and *PA4881*, which encodes a small tandem repeat protein (9, 66). To investigate whether MexT was activated in response to disulfide stress, expression levels from the *mexE*, *PA4354*, and *PA4881* promoter regions were determined in the presence and absence of subinhibitory concentrations of diamide. Three *lacZ* reporter fusions harboring the *mexE*, *PA4881*, and *PA4354* upstream promoter regions were introduced into PA14, and β-galactosidase activity was measured in the presence and absence of diamide. Induction levels were assayed at 1/4 and 1/2 the MIC of diamide in PA14 (8 mM and 16 mM, respectively). All three MexT-regulated targets were induced by diamide in a concentration-dependent manner, with the highest level of induction observed at 1/2 the MIC of diamide (Fig. 2). Interestingly, the presence of diamide strongly inhibited phenazine production in bacterial cultures (see Fig. S3A in the supplemental material). This is consistent with the observed association between MexT activation and the repression of quorum sensing-regulated virulence factors (24, 29). In addition, the presence of diamide caused increased resistance to chloramphenicol, in further correlation with its associated induction of MexEF-OprN (see Fig. S3B in the supplemental material).

**Oxidized MexT forms an oligomeric complex.** Oxidation of LTTRs is a proposed mechanism of transcriptional activation and deactivation in response to oxidative stress signals whereby a subset of LTTRs form oligomeric complexes when oxidized, leading to modulation of target gene expression (1, 58, 72). As MexT was demonstrated to be activated by diamide, which shifts the cellular redox environment toward a more oxidizing state, we hypothesized that MexT could form an active oligomeric complex under oxidizing conditions. In agreement with this, purified MexT protein was visualized as a monomer of ~35 kDa under reducing conditions with DTT, while under oxidizing conditions, formation of an oligomer which migrated to a position corresponding to ~100 kDa was clearly evident (Fig. 3). Increasing concentrations of reduced glutathione (GSH) decreased oligomer formation while inducing monomer formation (Fig. 4). In contrast, MexT oligomerization was increased under oxidizing conditions in samples treated with oxidized glutathione (GSSG). The redox potential of MexT was calculated by a previously described redox titration method (1, 72). The redox potential of MexT was determined to be −189 mV, assuming formation of a tetrameric complex. Such a high redox potential would ensure that MexT remains in a reduced and inactive state under the reducing conditions of the cytoplasm, which has an estimated redox potential of approximately −280 mV in *E. coli* (43, 57).

**Oxidation increases MexT binding to target promoters.** The observations that MexT target promoters are induced in the presence of diamide and that MexT forms an oligomeric complex under oxidative conditions suggested that the oligomeric form of

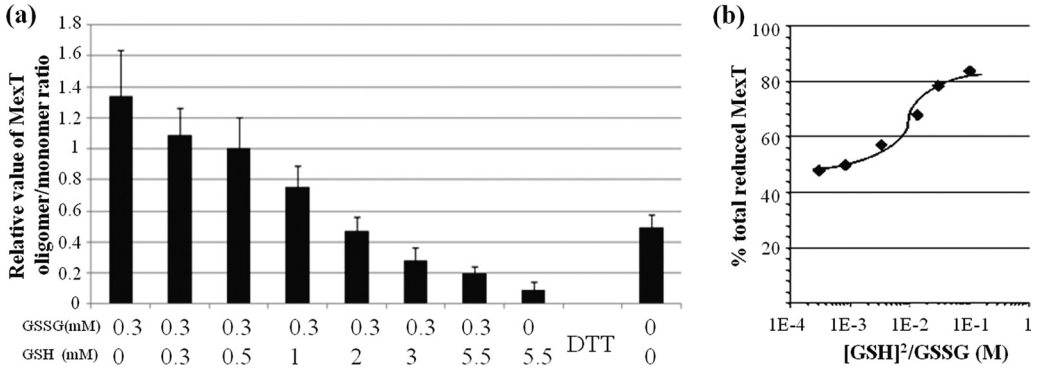


**FIG 4** Determination of MexT redox potential. (a) Various concentrations of GSH and GSSH were incubated with 20 ng of purified His-tagged MexT protein. Proteins were analyzed by nonreducing denaturing SDS-PAGE, and the MexT oligomer/monomer ratio was quantified in response to alteration of the GSSG/GSH ratio as well as in the presence of DTT and in the absence of oxidizing or reducing agents. (b) The percentage of reduced MexT was plotted on a titration curve against the known experimental concentrations of GSH and GSSH, assuming a four-monomer oxidation of MexT as described in equation 1 (70). Black diamonds represent experimentally determined data points, and the solid line represents the theoretical fit of the data according to equation 1. The redox potential of MexT was calculated to be −189 mV by application of the Nernst equation (70).

MexT represents its active state. To validate this assumption, MexT binding to the *PA4881* promoter, within which the presence of a MexT binding site has been demonstrated at the molecular level (66), was investigated by electrophoretic mobility shift assays (EMSA). MexT-promoter binding was assessed under oxidizing and reducing conditions similar to those under which oligomerization was observed. In agreement with our prediction, increasing the oxidation state of MexT in the presence of an excess of GSSG led to increased promoter binding, whereas reducing conditions abrogated MexT-promoter binding (Fig. 5). This provides further *in vitro* evidence that MexT activates its target genes as an oxidized oligomeric complex, in line with its proposed role as a redox-responsive regulator of disulfide stress.

**Disruption of *mexS* leads to changes in the cellular redox state.** MexT is activated by diamide and mediates resistance to this compound via induction of MexEF-OprN. Thus, it is likely that the thiol-disulfide redox imbalances induced by diamide mimic the conditions under which MexT is activated *in vivo*. In *nfxC*-type strains, including PA14*nfxC*, inactivating mutations in the *mexS* gene lead to constitutive activation of MexT (38, 60). The PA14*nfxC* strain used in this study harbors a nonsynonymous mutation (G160T), which introduces a premature stop codon in *mexS*. This strain exhibits classical features associated with *nfxC* phenotypic mutants, including increased chloramphenicol resistance and reduced phenazine production, which are complemented by introduction of a functional copy of *mexS* (see Fig. S4 in the supplemental material). We postulated that mutational disruption of *mexS* results in redox imbalances analogous to those induced by the presence of diamide, which trigger activation of MexT in PA14.

To investigate whether inactivation of *mexS* impacted upon the cellular redox status of PA14*nfxC*, the TV redox quantification assay was performed (64). Quantification of formazan production in PA14 and the *mexS* mutant strain PA14*nfxC* revealed that TV reduction was significantly lower (~40%) in cells of PA14*nfxC* than in PA14 (Fig. 6). A decrease in formazan production reflects depletion of reducing equivalents and signifies redox imbalances characteristic of cells experiencing oxidative stress (64). The observed decrease in formazan production relative to PA14 was restored on introduction of a functional *mexS* gene into PA14*nfxC*. This implicated redox imbalances associated with inactivation of

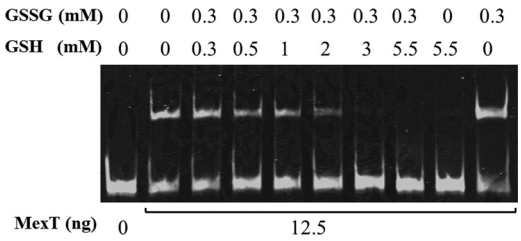


**FIG 5** MexT exhibits increased target promoter binding under oxidizing conditions. EMSAs were performed using the infrared-labeled *PA4881* promoter region (10 fmol) as a probe and 12.5 ng of the purified His-tagged MexT protein in the presence of various concentrations of GSH and GSSG. Incubation of MexT protein with DNA probe in the presence of increasing concentrations of GSH abrogated binding of MexT to the *PA4881* promoter region.

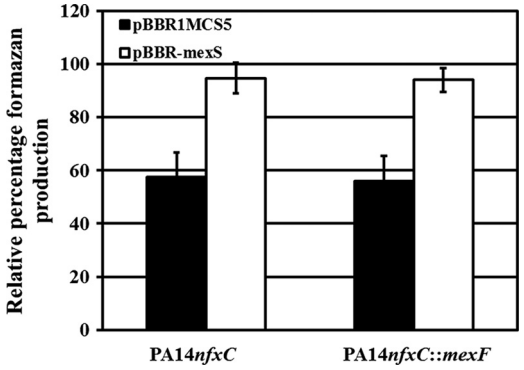


**FIG 6** Disruption of *mexS* mediates changes in the cellular redox environment in PA14*nfxC*. The percentage of TV reduction to formazan relative to PA14 was determined in growing cells of PA14*nfxC* and PA14*nfxC*::*mexF*. The formazan production results are expressed as mean percentage formazan production relative to PA14 ± the standard deviation of three independent experiments for each strain. Student's *t* test was performed and confirmed a highly significant (~40%) reduction in formazan production in both PA14*nfxC* and PA14*nfxC*::*mexF* ($P < 0.05$). Complementation of the *mexS* mutation in both PA14*nfxC* and PA14*nfxC*::*mexF* by introduction of the pBBR-mexS complementation construct restored TV reduction rates to wild-type PA14 levels in both strains.

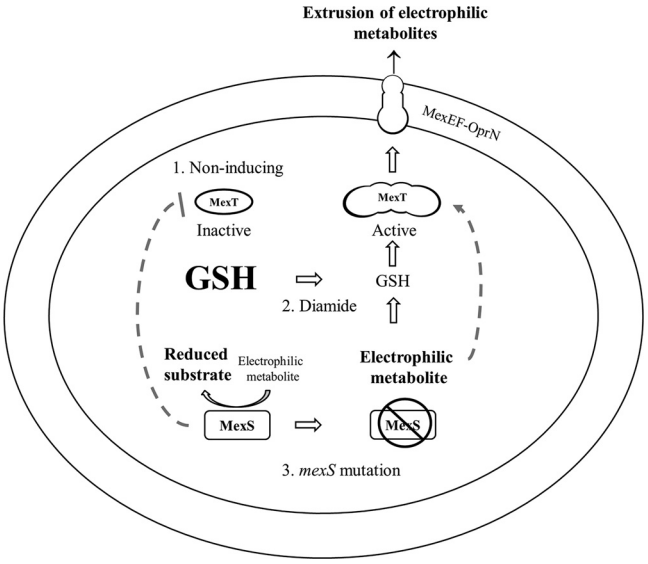


**FIG 7** Proposed model for MexT-mediated redox control in *P. aeruginosa*. (1) MexT remains in a reduced, monomeric form due to its high redox potential relative to the reducing environment of the cytoplasm. Under noninducing conditions, redox homeostasis is proposed to be maintained by MexS via reduction of an electrophilic metabolite. In the presence of diamide (2), the level of reduced glutathione (GSH) in the cytoplasm is rapidly depleted. This can alter the redox environment of the cytoplasm and facilitate the oxidation of MexT. Inactivation of *mexS* (3) alters the cellular redox environment which likely results from the accumulation of the electrophilic *mexS* substrate. Thus, an increase in the concentration of electrophilic molecules such as diamide or the natural *mexS* substrate favors the activation of MexT, leading to the induction of MexEF-OprN and the extrusion of such compounds or in an attempt to restore redox homeostasis.

*mexS* as an activating stimulus for MexT. Complementation of formazan reduction rates by *mexS* was also observed in PA14*nfxC*::*mexF*, illustrating the independence of *mexS*-mediated redox changes on the MexF RND efflux pump (Fig. 6). This ruled out the possibility that the changes in formazan reduction rates are caused by MexEF-OprN-mediated efflux of TV as observed for other redox probes (68). In addition, TV sensitivity levels were comparable between PA14, PA14::*mexF*, PA14::*mexT*, and PA14*nfxC*, which further suggests that TV is not a MexEF-OprN substrate (data not shown). Taken together, these observations support a model whereby *mexS* contributes as a biological modulator of the cellular redox status through its ability to reduce electrophilic metabolites. The buildup of such compounds (as may occur when *mexS* is mutated) impacts upon the redox environment of the cell, which leads to the activation of MexT and induction of MexEF-OprN, presumably in an attempt to restore redox homeostasis via efflux of unwanted electrophilic compounds (Fig. 7).

## DISCUSSION

This study identified a novel role for MexT as a regulator of intrinsic disulfide-stress resistance in *P. aeruginosa*. Although a number of compounds are known to activate MexT, diamide represents the first such molecule for which a corresponding resistance phenotype has been demonstrated. Chloramphenicol resistance, for example, is associated with induction of the MexEF-OprN efflux system, which is induced together with other MexT-activated targets (9, 23). However, deletion of MexT does not confer chloramphenicol susceptibility (see Fig. S1 in the supplemental material). Thus, while it has been demonstrated that MexT may contribute to chloramphenicol resistance in antibiotic-resistant mutants via its activation of MexEF-OprN, it does not mediate *intrinsic* resistance to chloramphenicol. Similarly, MexT is activated by *S*-nitrosoglutathione (GNSO) but does not appear to protect the cell from the toxic effects of this nitrosative stress elicitor (9).

Although induction of MexEF-OprN is linked to resistance to several antibacterial compounds, it remains to be demonstrated whether these compounds (e.g., unmodified chloramphenicol or diamide) are the transported substrates of this pump. In addition to efflux, the modification of chloramphenicol by chloramphenicol transacetylase is an established resistance mechanism which is observed in clinical pathogens, including *P. aeruginosa* (18, 47). It may be that MexEF-OprN transports modified adducts of chloramphenicol, diamide, or other foreign or unwanted molecules. Indeed, acetylation has been implicated as a general tagging process to promote the efflux of unwanted molecules, such as chloramphenicol, which are subsequently exported (5). However, diamide should inhibit this process, as transacetylation involves coenzyme A, which can form adducts with many sulfide-containing molecules and would be highly sensitive to diamide-mediated sulfur oxidation (3, 39). Hence, diamide should cause increased chloramphenicol susceptibility, but in fact, the opposite occurs in *P. aeruginosa*, as MexEF-OprN is induced in its presence (see Fig. S3B in the supplemental material). Given this discrepancy, acetylation-mediated tagging of chloramphenicol for export via MexEF-OprN would appear unlikely. This is further supported by the observation that *mexT* disruption causes increased diamide susceptibility in PA14::*mexT*, whereas chloramphenicol sensitivity is unaltered in this strain. Thus, the activation of MexT by diamide rather than chloramphenicol may more closely mimic the conditions under which MexT is activated *in vivo*, implicating MexT as a redox-responsive regulator within the intrinsic disulfide stress resistance pathway of *P. aeruginosa*.

Several studies have demonstrated the role of MexT in mediating MexEF-OprN induction in antibiotic-resistant mutants (19, 23, 60). However, this is the first report to identify a phenotype linked to the disruption of *mexT* in a wild-type background where MexEF-OprN is not constitutively induced. A targeted survey of the PA14 NR library confirmed that the contribution of *mexF* to intrinsic diamide resistance is unique among the RND pumps encoded in PA14. However, as several pumps have overlapping antibiotic resistance profiles, it remains to be determined whether other RND efflux systems could confer resistance to diamide when overexpressed or whether this is a unique feature of MexEF-OprN (37). Somewhat surprisingly, disruption of the *oprN* gene (encoding the outer membrane component of the MexEF-OprN system) had only a marginal effect on diamide sensitivity. This suggests that it is the extrusion of diamide from the cytoplasm via MexF that largely accounts for MexT-mediated diamide resistance. This may reflect the toxic properties of diamide, which stem from its ability to deplete cytoplasmic glutathione, leading to unfavorable distortions of the cytoplasmic redox environment (25, 58). The influence of an RND family efflux pump on the MIC of toxic substrates is dependent not only on the kinetic parameters of the efflux process but also upon the ability of the compound to permeate the outer membrane (35). This suggests that diamide can permeate the outer membrane and that it is primarily cyto-

plasmic extrusion driven by MexF that offsets its toxic effects on the cell.

In contrast, natural MexEF-OprN substrates might be excluded by the outer membrane, and hence OprN might contribute more significantly to protection against such molecules. Individual RND efflux pumps may form tripartite systems with diverse porins, and MexF could potentially extrude diamide via an alternative porin (50). However, interrogation of mutants from the PA14 NR library did not implicate any known RND-associated outer membrane porins in diamide resistance. Furthermore, in a Tn*5* mutagenesis screen to find genes contributing to chloramphenicol resistance in PA14*nfxC*, *oprN* was the only outer membrane porin gene identified. Similarly to diamide, chloramphenicol resistance exhibited only partial dependence on OprN. In addition to diamide and chloramphenicol resistance, repression of phenazine production in PA14*nfxC* also exhibited independence on OprN (see Fig. S2 in the supplemental material). This would suggest that in addition to diamide and chloramphenicol, efflux of certain endogenous MexEF-OprN substrates can also exhibit independence on OprN. Indeed, as OprN is an outer membrane channel, it could facilitate initial uptake of yet-unidentified metabolites whose resultant breakdown products are toxic. Such compounds may subsequently require extrusion from the cytoplasm by MexF via a MexT-dependent signal transduction cascade.

The induction of MexT-regulated targets by diamide confirmed the role of MexT in responding to diamide-induced stress signals, providing further insight into MexT activation. Diamide-mediated oxidation of glutathione proceeds readily in the cell, lowering the available level of reduced glutathione and causing imbalances in the thiol-disulfide redox state (25, 58). In such an environment the formation of aberrant disulfide bonds and glutathione adducts could play a role in the activation of MexT. Indeed, the addition of exogenous GNSO (a glutathione adduct), which accumulates under conditions of nitrosative stress, leads to MexT activation in *P. aeruginosa* (9). Glutathione adducts generated in the presence of compounds such as methylglyoxal, *N*-ethyl maleimide, or electrophilic quinones have also been demonstrated to serve as inducing signals for the potassium efflux system (Kef) in *Escherichia coli*, which offers protection against electrophilic compounds (40, 44). Likewise, specific glutathione adducts which accumulate in the presence of diamide could serve as activating signals for MexT, triggering induction of MexEF-OprN.

The observation that an oligomeric complex is formed by purified MexT protein under oxidizing conditions is in line with the LTTR paradigm, as classical LTTRs such as OxyR form active tetramers in response to their cognate inducing signals (2, 27). The calculated redox potential of MexT suggests that MexT remains in a reduced, monomeric form under normal physiological conditions in the absence of oxidative stressors, in line with MexT's role as a redox-responsive regulator. The fact that mutational disruption of *mexS* leads to constitutive activation of MexT functionally links this predicted oxidoreductase to MexT activation (60). It also implies that the natural MexT-activating ligand is produced by *P. aeruginosa*, possibly an electrophilic substrate of MexS. The recently described redox-responsive sensor kinase MtxR, reported during the preparation of the manuscript to negatively influence MexT activation, may also be involved in this signal transduction process and further implicates MexT in redox signaling (71).

MexS is a member of the MDR2 family (medium-chain dehydrogenases/reductase [MDR]/zinc-dependent alcohol dehydrogenase-like family) within the Conserved Domains Database (43). Accordingly, MexS shares homology with several MDR2 proteins, some of which are known to function in the detoxification of electrophilic compounds. Although proteins in the MDR2 family can function as reductases or dehydrogenases, our findings provide indirect evidence that MexS functions as a reductase in maintaining cellular redox balance. As such, MexS may function in a similar manner to NADPH-dependent soluble zeta-crystallin-like quinone oxidoreductases within the MDR2 family, which reduce not only quinones but also other electrophiles, including 2-alkenals and diamide (42, 49, 65). Our data support a model whereby disruption of *mexS* in *nfxC* mutants leads to the accumulation of the cognate MexS substrate, which, in turn, leads to redox imbalances in the cytoplasm, favoring the oxidation and thus activation of MexT. Recently, it has been demonstrated that the MexS-MexT signal transduction cascade may involve direct protein-protein interaction between MexS and MexT (19). A similar interaction has been observed in *Sphingomonas macrogoltabidus*, where the ThnY ferredoxin reductase-like iron-sulfur flavoprotein directly interacts with the ThnR LTTR in controlling expression of genes involved in tetralin biodegradation (12). Interestingly, ThnY and ThnR are also purported to transduce metabolic redox signals emerging from the tetralin catabolic pathway. Thus, the interaction with metabolic enzymes such as ThnY and MexS may represent an important mechanism of signal transduction among redox-responsive LTTRs. While overexpression of MexS had no impact on TV reduction in PA14 (data not shown), overexpression of MexS in PA14*nfxC* restored TV reduction rates to wild-type levels. Significantly, complementation of the *mexS*-linked TV reduction phenotype exhibited independence on *mexF*, demonstrating that MexS itself can impact the redox environment of the cell. Thus, MexS-associated redox imbalances induce MexEF-OprN via MexT in an apparent attempt to restore redox balance through efflux of electrophilic metabolites (Fig. 7).

Induction of MexEF-OprN likely leads to the extrusion of exogenous metabolites whose accumulation in the cell triggers induction via a MexS-MexT-linked signal transduction cascade. However, the precise nature of these activating compounds remains to be determined. The *Pseudomonas* quinolone signaling molecule precursor 4-hydroxy-2-heptylquinoline (HHQ) was recently identified as a potential substrate of MexEF-OprN, suggesting that electrophilic intermediates of 4-quinolone or quinoline biosynthesis may represent the natural substrates of MexEF-OprN. Indeed, the MexGHI-OpmD efflux system has been demonstrated to protect *P. aeruginosa* from endogenously produced phenazine pyocyanin, which induces MexGHI-OpmD via the redox-responsive regulator SoxR (6, 7, 54). Likewise, MexT may also function as a redox-responsive regulator mediating intrinsic resistance to redox-active secondary metabolites via induction of MexEF-OprN. While the manuscript was in preparation, the extrusion of kynurenine by MexEF-OprN was also demonstrated and shown to impact the growth of the PAO1 MexEF-OprN-overexpressing mutant PT149 on HHQ, kynurenine, or tryptophan as a sole carbon source (48). Hence, MexEF-OprN can extrude diverse, endogenously produced metabolites when active. However, whether this is the "intended" function of MexEF-OprN or simply a consequence of inappropriate efflux remains an open question (32, 62). As MexT-mediated induction of MexEF-OprN is linked to the metabolic function of MexS, future work in this area must

focus on identifying the endogenous substrates of MexS. These substrates or their modified derivatives are likely the true biological substrates of MexEF-OprN. Therefore, MexT and MexEF-OprN must be expected to mediate some observable protection from these metabolites, which should also trigger induction of MexEF-OprN via MexT's redox-sensory function in correlation with our observations for diamide. The observation that MexT confers intrinsic diamide resistance in PA14 provides a tractable system to dissect further the redox signaling cascade involving MexS, MexT, and the recently identified MtxR and its relationship to MexEF-OprN induction, virulence, and antibiotic and disulfide stress resistance in *P. aeruginosa*.

## ACKNOWLEDGMENTS

We thank Pat Higgins for excellent technical assistance.

This research was supported in part by grants awarded by the European Commission (MTKD-CT-2006-042062; O36341), the Science Foundation of Ireland (SFI 02/IN.I/B1261 and 04/BR/B0597), the Department of Agriculture and Food (DAF RSF 06 321 and DAF RSF 06 377), the Irish Research Council for Science, Engineering and Technology (IRCSET) (05/EDIV/FP107), the Health Research Board (RP/2004/145, RP/2006/271, and RP/2007/290), the Environmental Protection Agency (EPA 2006-PhD-S-21), and the Higher Education Authority of Ireland (PRTLI3).

## REFERENCES

1. **Chen H, et al.** 2008. The Pseudomonas aeruginosa multidrug efflux regulator MexR uses an oxidation-sensing mechanism. Proc. Natl. Acad. Sci. U. S. A. **105**:13586–13591.
2. **Choi H, et al.** 2001. Structural basis of the redox switch in the OxyR transcription factor. Cell **105**:103–113.
3. **Collier GE, Nishimura JS.** 1978. Affinity labeling of succinyl-CoA synthetase from porcine heart and Escherichia coli with oxidized coenzyme A disulfide. J. Biol. Chem. **253**:4938–4943.
4. **Cosson P, et al.** 2002. Pseudomonas aeruginosa virulence analyzed in a Dictyostelium discoideum host system. J. Bacteriol. **184**:3027–3033.
5. **Danchin A.** 2009. Cells need safety valves. Bioessays **31**:769–773.
6. **Dietrich LE, Price-Whelan A, Petersen A, Whiteley M, Newman DK.** 2006. The phenazine pyocyanin is a terminal signalling factor in the quorum sensing network of Pseudomonas aeruginosa. Mol. Microbiol. **61**: 1308–1321.
7. **Dietrich LE, Teal TK, Price-Whelan A, Newman DK.** 2008. Redox-active antibiotics control gene expression and community behavior in divergent bacteria. Science **321**:1203–1206.
8. **Favre-Bonté S, Kohler T, Van Delden C.** 2003. Biofilm formation by Pseudomonas aeruginosa: role of the C4-HSL cell-to-cell signal and inhibition by azithromycin. J. Antimicrob. Chemother. **52**:598–604.
9. **Fetar H, et al.** 2011. mexEF-oprN multidrug efflux operon of Pseudomonas aeruginosa: regulation by the MexT activator in response to nitrosative stress and chloramphenicol. Antimicrob. Agents Chemother. **55**:508–514.
10. **Figurski DH, Helinski DR.** 1979. Replication of an origin-containing derivative of plasmid RK2 dependent on a plasmid function provided in trans. Proc. Natl. Acad. Sci. U. S. A. **76**:1648–1652.
11. **Frisk A, et al.** 2004. Transcriptome analysis of Pseudomonas aeruginosa after interaction with human airway epithelial cells. Infect. Immun. **72**: 5433–5438.
12. **Garcia LL, et al.** 2011. ThnY is a ferredoxin reductase-like iron-sulfur flavoprotein that has evolved to function as a regulator of tetralin biodegradation gene expression. J. Biol. Chem. **286**:1709–1718.
13. **Gibson RL, Burns JL, Ramsey BW.** 2003. Pathophysiology and management of pulmonary infections in cystic fibrosis. Am. J. Respir. Crit. Care Med. **168**:918–951.
14. **Gooderham WJ, Hancock RE.** 2009. Regulation of virulence and antibiotic resistance by two-component regulatory systems in Pseudomonas aeruginosa. FEMS Microbiol. Rev. **33**:279–294.
15. **Hauser AR.** 2009. The type III secretion system of Pseudomonas aeruginosa: infection by injection. Nat. Rev. Microbiol. **7**:654–665.
16. **Heeb S, et al.** 2000. Small, stable shuttle vectors based on the minimal pVS1 replicon for use in gram-negative, plant-associated bacteria. Mol. Plant Microbe Interact. **13**:232–237.
17. **Hirai K, Suzue S, Irikura T, Iyobe S, Mitsuhashi S.** 1987. Mutations producing resistance to norfloxacin in Pseudomonas aeruginosa. Antimicrob. Agents Chemother. **31**:582–586.
18. **Ingram JM, Hassan HM.** 1975. The resistance of Pseudomonas aeruginosa to chloramphenicol. Can. J. Microbiol. **21**:1185–1191.
19. **Jin Y, Yang H, Qiao M, Jin S.** 2011. MexT regulates the type III secretion system through MexS and PtrC in Pseudomonas aeruginosa. J. Bacteriol. **193**:399–410.
20. **Jones RN.** 2010. Microbial etiologies of hospital-acquired bacterial pneumonia and ventilator-associated bacterial pneumonia. Clin. Infect. Dis. **51**(Suppl 1):S81–S87.
21. **Juhas M, Eberl L, Tummler B.** 2005. Quorum sensing: the power of cooperation in the world of Pseudomonas. Environ. Microbiol. **7**:459–471.
22. **Kallifidas D, Thomas D, Doughty P, Paget MS.** 2010. The sigmaR regulon of Streptomyces coelicolor A32 reveals a key role in protein quality control during disulphide stress. Microbiology **156**:1661–1672.
23. **Köhler T, Epp SF, Curty LK, Pechere JC.** 1999. Characterization of MexT, the regulator of the MexE-MexF-OprN multidrug efflux system of Pseudomonas aeruginosa. J. Bacteriol. **181**:6300–6305.
24. **Köhler T, van Delden C, Curty LK, Hamzehpour MM, Pechere JC.** 2001. Overexpression of the MexEF-OprN multidrug efflux system affects cell-to-cell signaling in Pseudomonas aeruginosa. J. Bacteriol. **183**:5213–5222.
25. **Kosower NS, Kosower EM.** 1995. Diamide: an oxidant probe for thiols. Methods Enzymol. **251**:123–133.
26. **Kovach ME, et al.** 1995. Four new derivatives of the broad-host-range cloning vector pBBR1MCS, carrying different antibiotic-resistance cassettes. Gene **166**:175–176.
27. **Kullik I, Stevens J, Toledano MB, Storz G.** 1995. Mutational analysis of the redox-sensitive transcriptional regulator OxyR: regions important for DNA binding and multimerization. J. Bacteriol. **177**:1285–1291.
28. **Kumar A, Schweizer HP.** 2011. Evidence of MexT-independent overexpression of MexEF-OprN multidrug efflux pump of Pseudomonas aeruginosa in presence of metabolic stress. PLoS One **6**:e26520. doi:10.1371/journal.pone.0026520.
29. **Lamarche MG, Deziel E.** 2011. MexEF-OprN efflux pump exports the Pseudomonas quinolone signal (PQS) precursor HHQ (4-hydroxy-2-heptylquinoline). PLoS One **6**:e24310. doi:10.1371/journal.pone.0024310.
30. **Leichert LI, Scharf C, Hecker M.** 2003. Global characterization of disulfide stress in Bacillus subtilis. J. Bacteriol. **185**:1967–1975.
31. **Lewenza S, et al.** 2005. Construction of a mini-Tn5-luxCDABE mutant library in Pseudomonas aeruginosa PAO1: a tool for identifying differentially regulated genes. Genome Res. **15**:583–589.
32. **Li XZ, Nikaido H.** 2009. Efflux-mediated drug resistance in bacteria: an update. Drugs **69**:1555–1623.
33. **Liberati NT, et al.** 2006. An ordered, nonredundant library of Pseudomonas aeruginosa strain PA14 transposon insertion mutants. Proc. Natl. Acad. Sci. U. S. A. **103**:2833–2838.
34. **Liebeke M, et al.** 2008. Depletion of thiol-containing proteins in response to quinones in Bacillus subtilis. Mol. Microbiol. **69**:1513–1529.
35. **Lim SP, Nikaido H.** 2010. Kinetic parameters of efflux of penicillins by the multidrug efflux transporter AcrAB-TolC of Escherichia coli. Antimicrob. Agents Chemother. **54**:1800–1806.
36. **Linares JF, et al.** 2005. Overexpression of the multidrug efflux pumps MexCD-OprJ and MexEF-OprN is associated with a reduction of type III secretion in Pseudomonas aeruginosa. J. Bacteriol. **187**:1384–1391.
37. **Lister PD, Wolter DJ, Hanson ND.** 2009. Antibacterial-resistant Pseudomonas aeruginosa: clinical impact and complex regulation of chromosomally encoded resistance mechanisms. Clin. Microbiol. Rev. **22**:582–610.
38. **Llanes C, et al.** 2011. Role of the MexEF-OprN efflux system in low-level resistance of Pseudomonas aeruginosa to ciprofloxacin. Antimicrob. Agents Chemother. **55**:5676–5684.
39. **Loewen PC.** 1977. Identification of a coenzyme A–glutathione disulfide (DSI), a modified coenzyme A disulfide (DSII), and a NADPH-dependent coenzyme A–glutathione disulfide reductase in E. coli. Can. J. Biochem. **55**:1019–1027.
40. **Lyngberg L, et al.** 2011. KefF, the regulatory subunit of the potassium

efflux system KefC, shows quinone oxidoreductase activity. J. Bacteriol. **193**:4925–4932.
41. **Maddocks SE, Oyston PC.** 2008. Structure and function of the LysR-type transcriptional regulator (LTTR) family proteins. Microbiology **154**: 3609–3623.
42. **Mano J, et al.** 2002. The NADPH:quinone oxidoreductase P1-zeta-crystallin in Arabidopsis catalyzes the alpha,beta-hydrogenation of 2-alkenals: detoxication of the lipid peroxide-derived reactive aldehydes. Plant Cell Physiol. **43**:1445–1455.
43. **Marchler-Bauer A, et al.** 2011. CDD: a conserved domain database for the functional annotation of proteins. Nucleic Acids Res. **39**:D225–D229.
44. **McLaggan D, Rufino H, Jaspars M, Booth IR.** 2000. Glutathione-dependent conversion of N-ethylmaleimide to the maleamic acid by Escherichia coli: an intracellular detoxification process. Appl. Environ. Microbiol. **66**:1393–1399.
45. **Miller JH.** 1972. Experiments in molecular genetics. Cold Spring Harbor Laboratory Press, Cold Spring Harbor, NY.
46. **Mooij MJ, et al.** 2010. Antibiotic selection leads to inadvertent selection of nfxC-type phenotypic mutants in Pseudomonas aeruginosa. Environ. Microbiol. Rep. **2**:461–464.
47. **Neu HC, Fu KP.** 1980. In vitro activity of chloramphenicol and thiamphenicol analogs. Antimicrob. Agents Chemother. **18**:311–316.
48. **Olivares J, et al.** 15 March 2012. Overproduction of the multidrug efflux pump MexEF-OprN does not impair Pseudomonas aeruginosa fitness in competition tests, but produces specific changes in bacterial regulatory networks. Environ. Microbiol. doi:10.1111/j.1462–2920.2012.02727.x.
49. **Pan X, Zhang H, Gao Y, Li M, Chang W.** 2009. Crystal structures of Pseudomonas syringae pv. tomato DC3000 quinone oxidoreductase and its complex with NADPH. Biochem. Biophys. Res. Commun. **390**:597–602.
50. **Piddock LJ.** 2006. Multidrug-resistance efflux pumps—not just for resistance. Nat. Rev. Microbiol. **4**:629–636.
51. **Pócsi I, et al.** 2005. Comparison of gene expression signatures of diamide, H2O2 and menadione exposed Aspergillus nidulans cultures–linking genome-wide transcriptional changes to cellular physiology. BMC Genomics **6**:182.
52. **Poole K.** 2005. Efflux-mediated antimicrobial resistance. J. Antimicrob. Chemother. **56**:20–51.
53. **Porrúa O, Platero AI, Santero E, Del Solar G, Govantes F.** 2010. Complex interplay between the LysR-type regulator AtzR and its binding site mediates atzDEF activation in response to two distinct signals. Mol. Microbiol. **76**:331–347.
54. **Price-Whelan A, Dietrich LE, Newman DK.** 2007. Pyocyanin alters redox homeostasis and carbon flux through central metabolic pathways in Pseudomonas aeruginosa PA14. J. Bacteriol. **189**:6372–6381.
55. **Ruangprasert A, Craven SH, Neidle EL, Momany C.** 2010. Full-length structures of BenM and two variants reveal different oligomerization schemes for LysR-type transcriptional regulators. J. Mol. Biol. **404**:568–586.
56. **Schell MA.** 1993. Molecular biology of the LysR family of transcriptional regulators. Annu. Rev. Microbiol. **47**:597–626.
57. **Schell MA, Brown PH, Raju S.** 1990. Use of saturation mutagenesis to localize probable functional domains in the NahR protein, a LysR-type transcription activator. J. Biol. Chem. **265**:3844–3850.
58. **Smirnova GV, Oktyabrsky ON.** 2005. Glutathione in bacteria. Biochemistry (Mosc.) **70**:1199–1211.
59. **Smith EE, et al.** 2006. Genetic adaptation by Pseudomonas aeruginosa to the airways of cystic fibrosis patients. Proc. Natl. Acad. Sci. U. S. A. **103**: 8487–8492.
60. **Sobel ML, Neshat S, Poole K.** 2005. Mutations in PA2491 (mexS) promote MexT-dependent mexEF-oprN expression and multidrug resistance in a clinical strain of Pseudomonas aeruginosa. J. Bacteriol. **187**:1246–1253.
61. **Spaink HP, Okker RJH, Wijffelman CA, Pees E, Lugtenberg BJJ.** 1987. Promoters in the nodulation region of the Rhizobium leguminosarum Sym plasmid pRL1J1. Plant Mol. Biol. **9**:27–39.
62. **Stickland HG, Davenport PW, Lilley KS, Griffin JL, Welch M.** 2010. Mutation of nfxB causes global changes in the physiology and metabolism of Pseudomonas aeruginosa. J. Proteome Res. **9**:2957–2967.
63. **Stover CK, et al.** 2000. Complete genome sequence of Pseudomonas aeruginosa PAO1, an opportunistic pathogen. Nature **406**:959–964.
64. **Tachon S, et al.** 2009. Experimental conditions affect the site of tetrazolium violet reduction in the electron transport chain of Lactococcus lactis. Microbiology **155**:2941–2948.
65. **Thorn JM, Barton JD, Dixon NE, Ollis DL, Edwards KJ.** 1995. Crystal structure of Escherichia coli QOR quinone oxidoreductase complexed with NADPH. J. Mol. Biol. **249**:785–799.
66. **Tian ZX, et al.** 2009. Transcriptome profiling defines a novel regulon modulated by the LysR-type transcriptional regulator MexT in Pseudomonas aeruginosa. Nucleic Acids Res. **37**:7546–7559.
67. **Tian ZX, et al.** 2009. MexT modulates virulence determinants in Pseudomonas aeruginosa independent of the MexEF-OprN efflux pump. Microb. Pathog. **47**:237–241.
68. **Vidal-Aroca F, Meng A, Minz T, Page MG, Dreier J.** 2009. Use of resazurin to detect mefloquine as an efflux-pump inhibitor in Pseudomonas aeruginosa and Escherichia coli. J. Microbiol. Methods **79**:232–237.
69. **Vinckx T, Wei Q, Matthijs S, Cornelis P.** 2010. The Pseudomonas aeruginosa oxidative stress regulator OxyR influences production of pyocyanin and rhamnolipids: protective role of pyocyanin. Microbiology **156**: 678–686.
70. **Yeom S, Yeom J, Park W.** 2010. Molecular characterization of FinR, a novel redox-sensing transcriptional regulator in Pseudomonas putida KT2440. Microbiology **156**:1487–1496.
71. **Zaoui C, et al.** 2012. An orphan sensor kinase controls quinolone signal production via MexT in Pseudomonas aeruginosa. Mol. Microbiol. **83**: 536–547.
72. **Zheng M, Aslund F, Storz G.** 1998. Activation of the OxyR transcription factor by reversible disulfide bond formation. Science **279**:1718–1721.